

# Crack Growth Life Prediction in API 5L X46 Grade Steel Pipes Subjected to Cyclic Internal Pressure



S. Vishnuvardhan, A. Ramachandra Murthy, M. Saravanan, and P. Gandhi

## 1 Introduction

Oil and gas transportation pipelines experience cyclic pressure leading to failure by fatigue. Welded joints in the pipelines are the regions where fatigue cracks are expected to initiate and propagate due to increased stress concentration in view of inclusions and weld defects. In general, pipelines are prone to different failure modes such as plastic collapse by gross plastic deformation, fatigue failure due to cyclic internal pressure, buckling and post buckling instability under external pressure as well as interaction of stress corrosion and defects [1, 2]. The main problem associated with oil and gas transportation pipelines are (a) sweet corrosion, (b) sour corrosion and (c) microbiologically influence corrosion (MIC), which leads to pitting corrosion [3, 4]. Zheng et al. [5] studied the fatigue crack initiation life and the influence of pre-deformation on fatigue crack initiation life using single edge notch specimens machined from deformed X60 steel pipeline. Azevedo [6] investigated crack nucleation and propagation in API X46 grade crude oil pipeline and found that the crack nucleation on the internal surface of the pipeline was promoted by the presence of welding defects and corrosion pits, and propagated in a stable manner in both longitudinal and radial direction and later along the heat affected zone of the pipeline. The nucleation of the primary crack was found to be promoted.

Liu et al. [7] proposed a finite element method and evaluated the fatigue life of X65 steel buried natural gas pipeline under cyclic internal pressure and vibrating loads. Liu et al. [8] conducted failure analysis on API X65 steel natural gas pipeline buried at a depth of 1200 mm with diameter and thickness of 813 and 12.5 mm and predicted the load-bearing capacity of the pipeline by 3D finite element analysis using ABAQUS. Hasan et al. [9] studied the failure of an 18-inch diameter gas pipeline caused by

---

S. Vishnuvardhan (✉) · A. Ramachandra Murthy · M. Saravanan · P. Gandhi  
CSIR—Structural Engineering Research Centre, Chennai 600 113, India  
e-mail: [svvardhan@serc.res.in](mailto:svvardhan@serc.res.in)

stress corrosion cracking (SCC) influenced by the coal-tar based coating. Hamid Reza Hajibagheri et al. [10] carried out inspection of a 6-inch diameter seamless steel pipeline, which was primarily used for transmitting oil and was later repurposed for transmitting gas. Cracks up to a depth of 100  $\mu\text{m}$  were observed on the surface and propagated inwardly and no cracks of stress corrosion cracking (SCC) and hydrogen induced cracking (HIC) type were present. Nguyen et al. [11] conducted fracture toughness and fatigue crack growth rate (FCGR) tests on X70 pipeline steel base and weld metals under 10 MPa of a natural/hydrogen gas mixture with 1%  $\text{H}_2$  blend. A significant reduction in the fracture toughness and accelerated fatigue crack growth rates were observed in both the metals under the gas mixture with 1%  $\text{H}_2$  blend compared with the tests conducted in ambient air. Jiao and Shuai [12] conducted cyclic pressure studies on long distance transmission pipelines and it was observed that the cyclic pressure is one of the main reasons of pipeline damage. Rainflow counting method could be used to resolve the pressure cycles and an appropriate pipeline maintenance scheme could be adopted for considering the cyclic pressure.

Ghaednia et al. [13] studied the effect of crack depth on burst strength of X70 pipeline with combined dent-crack defect. It was observed that the combined dent-crack defect with crack depth of 75% of wall thickness could reduce the pressure capacity by 54%. A pipeline material fatigue crack growth database was developed using fatigue crack growth rate tests conducted on base and weld materials of different pipeline steel grades ranging from X46 to X70 under two different stress ratios. It was reported that the crack growth rates in the pipeline steels tested were two to three times lower than the crack growth rates recommended in BS 7910 [14]. Tewari and Agarwal [15] investigated the failure of an in-service pipeline. Pipeline failed from its longitudinal seam, failure initiated from heat affected zone (HAZ) when the pipeline was in operation. The failure occurred much below the maximum allowable operating pressure (MAOP) of the Pipeline. The pipeline was operating pressure at 77  $\text{kg}/\text{cm}^2$  against the MAOP was 91.4  $\text{kg}/\text{cm}^2$ . After examination, the pipe seam weld was reported to be affected by fatigue and that the failure might have initiated from a crack at the internal surface of the pipe.

In the present studies, crack growth life of API 5L X46 grade steel in-service pipes subjected to cyclic internal pressure was evaluated experimentally. Numerical studies were carried out on the pipes under cyclic internal pressure and stress intensity factor was evaluated by varying crack length and depth. SIF for different crack depths was also evaluated analytically using the expressions available in API 579/ASME FFS-1 and ASME B&PV Code Section XI Division I. Employing Paris' crack growth model and crack growth constants reported in the literature for API 5L X46 grade steel, number of cycles to failure was predicted both numerically and analytically.

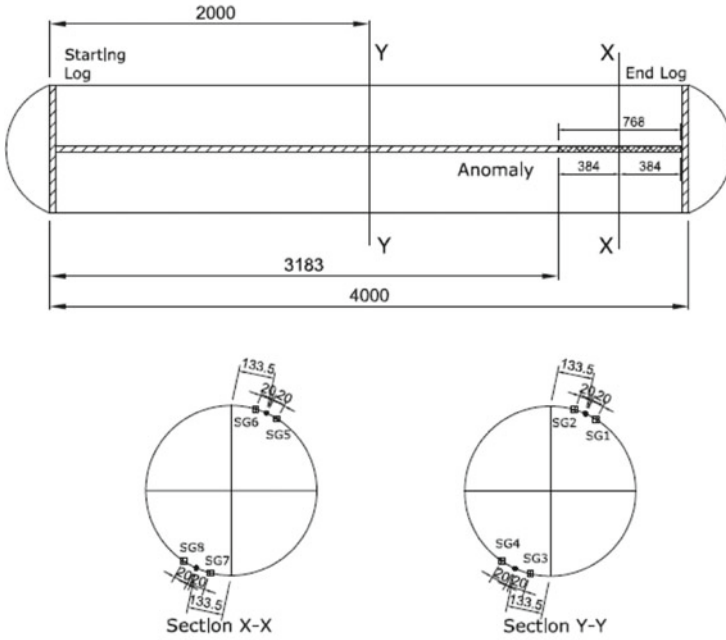
## 2 Details of Pipe Specimens

The pipe specimens used in the present studies were made of API 5L X46 Grade steel conforming to API 5L [16]. The pipe specimens of 4.0 m length with different defect profiles cut removed from in-service pipe line were used. The nominal outer diameter and thickness of the pipe specimens were 14" (355.6 mm) and 7.14 mm respectively. Based on the intelligent pigging measurements carried out in the field, one pipe was detected to contain a longitudinal seam crack of 32 mm length and 2 mm depth and the other pipe was detected to contain two lamination defects of different sizes. Length and width of one lamination was 644 mm and 121 mm respectively. Length and width of the other lamination was 967 mm and 228 mm respectively.

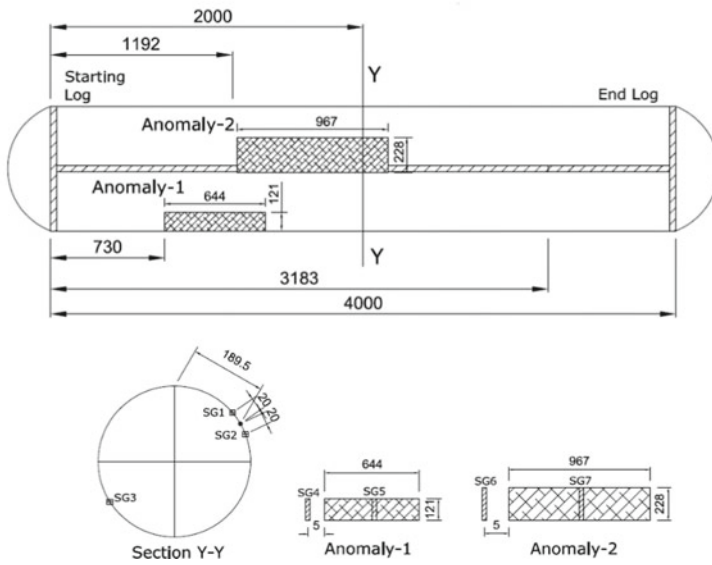
## 3 Experimental Studies

The pipe specimens were welded with curved blind flanges at both the ends. Two threadolets were provided in the pipe specimens at a distance of 200 mm from the weld centre. Threadolet is an opening given in the specimen with threads inside and a bolt is used for opening or closing it. This provision was used to fill the specimen with hydraulic oil and apply the desired internal pressure. The pipe specimens were instrumented with two element rosette strain gauges to study the variation of strains during cyclic pressure test. Strain gauges were mounted on the pipe specimen at two different cross-sections along the length of the pipe viz, centre of defect location and middle of pipe specimen. In the case of pipe specimen containing lamination defect, strain gages were also mounted at the edge of defect. Figure 1 shows details of pipe specimens, defect details and location of strain gauges.

The pipe specimens were filled with hydraulic oil and subjected to a cyclic pressure of 5–77 kg/cm<sup>2</sup> and then back to 5 kg/cm<sup>2</sup>. The pressure cycle simulates one day of actual operation in a typical oil pipeline in India. The cyclic pressure was applied on the pipe specimen using a slave hydraulic cylinder connected to the  $\pm 500$  kN capacity servo-hydraulic Universal Testing Machine. Figure 2 shows the set-up for cyclic pressure test on a pipe specimen. Figure 3 shows a typical pressure cycle. The rate of loading was one cycle per minute. The cyclic pressure tests were carried out till failure of the pipe specimens. During the cyclic pressure tests, load, load-line displacement and strains at different locations were monitored using a high-speed data acquisition system.



(a) Specimen with longitudinal seam crack



(b) Specimen with lamination defects

**Fig. 1** Details of pipe specimens, defect details and location of strain gauges

**Fig. 2** Set-up for cyclic pressure test on a pipe specimen

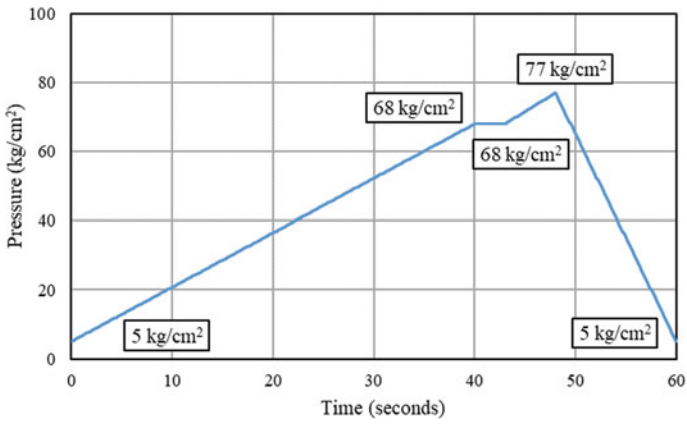


**Fig. 3** Typical pressure cycle

## 4 Numerical Studies

Numerical studies have also been carried out on pipe containing longitudinal seam crack under cyclic internal pressure and stress intensity factor values are evaluated. Pipe dimensions and crack details are same as the one that is used in experimental investigations. Both the ends of the pipe are considered to be fixed and the defect is modeled as internal elliptical crack. Centre of the crack is located at 1780 mm from one end of the pipe. Young's modulus and Poisson's ratio are taken as 200 GPa and 0.3 respectively. The pipe was subjected to cyclic pressure of 5–77 kg/cm<sup>2</sup> and then back to 5 kg/cm<sup>2</sup>. 3-D FEA is carried out to investigate the fracture behaviour of the pipe based on LEFM principles using eight noded solid elements with reduced integration (C3D8R). FE model is constructed with 54,400 elements and 98,646 nodes. Extended Finite Element Method (XFEM) is employed to carry out crack growth analysis. Stress intensity factor (SIF) was evaluated by varying crack length and depth using domain integral technique. SIF was evaluated at both the crack tips and also at the deepest point of the crack in the depth direction to understand the crack growth behaviour of the pipe.

## 5 Analytical Studies

Analytical prediction of remaining life of API 5L X 46 Grade steel pipes with different crack profiles subjected to internal pressure was carried out. Expressions available in API 579/ASME FFS-1 [17] and ASME B&PV Code Section XI Division I [18] were used to evaluate SIF corresponding to different values of crack depth, both at surface and deepest points.

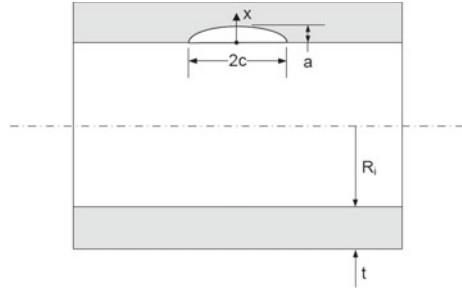
### 5.1 API 579-1/ASME FFS-1

As per API 579-1/ASME FFS-1, the Mode I stress intensity factor for a cylinder subjected to internal pressure with longitudinally oriented semi-elliptical surface crack (as shown in Fig. 4) can be computed by the following equations:

$$KI = pRo^2Ro^2 - Ri^2[2G0 - 2G1(aRi)^2 + 3G2(aRi)^3 - 4G3(aRi)^4 + 5G4(aRi)^5]\sqrt{\pi aQ} \quad (1)$$

where  $p$  is internal pressure,  $Ro$  is the external radius of the pipe,  $Ri$  is the internal radius of the pipe,  $a$  is the depth of crack and  $G0, G1, G2, G3, G4$  are the influence coefficients respectively. This equation is valid for  $0.0 \leq a/t \leq 0.8$  and  $0.0 \leq t/Ri \leq 1.0$ . The influence coefficients  $G0$  and  $G1$  for inside and outside surface cracks can

**Fig. 4** Mode I stress intensity factor for a cylinder subjected to internal pressure with longitudinally oriented semi-elliptical surface crack



be determined using the following equations:

$$G0 = A0.0 + A1.0\beta + A2.0\beta^2 + A3.0\beta^3 + A4.0\beta^4 + A5.0\beta^5 + A6.0\beta^6 \quad (2)$$

$$G1 = A0.1 + A1.1\beta + A2.1\beta^2 + A3.1\beta^3 + A4.1\beta^4 + A5.1\beta^5 + A6.1\beta^6 \quad (3)$$

where  $\beta = 2\phi\Pi$  and the parameters  $A_{ij}$  (i.e., the values from the row corresponding to  $G_i$  and the column  $A_j$ ) are for inside surface cracks and for outside surface cracks. The influence coefficients  $G2, G3, G4$  for inside and outside surface cracks at surface and deepest point of a semi-elliptical crack are derived as follows:

At deepest point ( $\phi = \pi/2$ ):

$$G2 = \sqrt{2Q\pi}(1615 + 13M1 + 16,105M2 + 112M3) \quad (4)$$

$$G3 = \sqrt{2Q\pi}(3235 + 14M1 + 32,315M2 + 120M3) \quad (5)$$

$$G4 = \sqrt{2Q\pi}(256,315 + 15M1 + 2,563,465M2 + 130M3) \quad (6)$$

where the weight function coefficients  $M1, M2, M3$  are calculated from the below equations:

$$M1 = 2\pi\sqrt{2}(3G1 - G0) - 245 \quad (7)$$

$$M2 = 3 \quad (8)$$

$$M3 = 6\pi\sqrt{2}(G0 - 2G1) - 85 \quad (9)$$

At surface point( $\phi = 0$ ),  $G2 = \sqrt{Q\pi}(45 + 23N1 + 47N2 + 12N3) \quad (10)$

$$G3 = \sqrt{Q\pi}(47 + 12N1 + 49N2 + 25N3) \quad (11)$$

$$G4 = \sqrt{Q\pi(49 + 25N1 + 411N2 + 13N3)} \tag{12}$$

where the weight function coefficients  $N1, N2, N3$  are calculated from the below equations:

$$N1 = 3\pi\sqrt{(2G0 - 5G1) - 8} \tag{13}$$

$$N2 = 15\pi\sqrt{(3G1 - G0) + 15} \tag{14}$$

$$N3 = 3\pi\sqrt{(3G0 - 10G1) - 8} \tag{15}$$

The elliptical shape factor  $Q$  is determined using  $Q = 1.0 + 1.464(ac)1.65$  for  $a/c \leq 1.0$  and  $Q = 1.0 + 1.464(ca)1.65$  for  $a/c > 1.0$

### 5.2 ASME Section XI

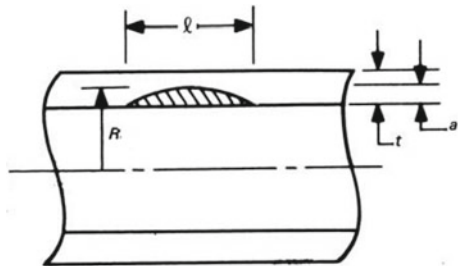
From paragraph H-4221.2 under Article H-4000 Screening criteria in ASME Boiler and Pressure Vessel Code (Section XI), Mode I stress intensity factor for a pressure vessel with semi-elliptical axial flow (as shown in Fig. 5) at the internal surface is given by the following equation:

$$K = (PRt)(\pi a Q)0.5F \tag{16}$$

where  $P$  is pressure inside the cylinder,  $R$  is the distance from the centre of the pipe to the deepest point of the semi-elliptical flaw,  $t$  is the thickness of the pipe,  $a$  and  $l$  are the depth and length of the crack respectively. The boundary correction factor  $F$  and the flaw shape parameter  $Q$  are determined by:

$$F = 1.12 + 0.053\alpha + 0.005\alpha^2 + (1.0 + 0.02\alpha + 0.0191\alpha^2)(20 - Rt)21,400 \tag{17}$$

**Fig. 5** Mode I stress intensity factor for a pressure vessel with semi-elliptical surface crack





$$Q = 1 + 4.593(\alpha)^{1.65} \quad (18)$$

where  $\alpha = (a/t)/(a/l)$ .

SIF values were obtained using the both the approaches for the pipe specimen with longitudinal seam crack in surface and as well as deepest point of crack. Crack growth analysis was carried out using the SIF values obtained employing Paris' crack growth equation. The analysis was carried out for every 0.5 mm crack depth till the value reached 5.5 mm, which is approximately 0.8 times the thickness of the pipe specimen. Crack length was assumed to increase by 2.5 mm for every 0.5 mm crack depth. Crack length corresponding to 5.5 mm crack depth was 49.5 mm.

## 6 Results and Discussion

Figure 6 shows typical strain versus time curves and Fig. 7 shows typical strain versus pressure curves for pipe specimen with longitudinal seam crack. Figure 8 shows typical strain versus time curves and Fig. 9 shows typical strain versus pressure curves for pipe specimen with lamination defects. It is observed that strain in the circumferential direction was higher compared to the longitudinal direction at a given location. The strain values are observed to be almost constant till the initiation of through-wall crack. It can be observed that the strain values close to the crack location increased rapidly just before the appearance of through-wall crack. In the case of pipe specimens with longitudinal seam crack, the existing crack had become through-wall and the specimen failed after completion of 1412 cycles indicating 3.87 years of remaining service life. Figure 10 shows close-up view of failure of pipe specimen with longitudinal seam crack. The pipe specimen with lamination defects has developed a through-wall crack and failed after completion of 2010 cycles indicating 5.51 years of remaining service life. Figure 11 shows close-up view of failure of pipe specimen with lamination defect.

Figure 12 shows stress distribution of ahead of crack tip. It was observed that the SIF is higher for the crack tip located nearer to the support than for the crack tip located away from the support due to the geometrical constraint effect of the crack position. Figure 13 shows SIF versus crack depth. As expected, SIF increased with increase in crack depth. Both the axial and von-Mises distributions are exhibited the fracture behaviour based on the material yield zone. It was observed that the crack tip located nearer to the support reached the yield first than the crack tip located away from the support, which could be due to the geometrical constraints and the boundary conditions.

Figure 14a shows SIF for different values of crack length and Fig. 14b shows SIF for different values of crack depth obtained using API 579/ASME FFS-1 for the pipe specimen with longitudinal seam crack. Figure 15 shows comparison of SIF obtained using API 579/ASME FFS-1 and ASME B&PV Code Section XI Division I. SIF value obtained at deepest point of crack was always higher compared to surface point

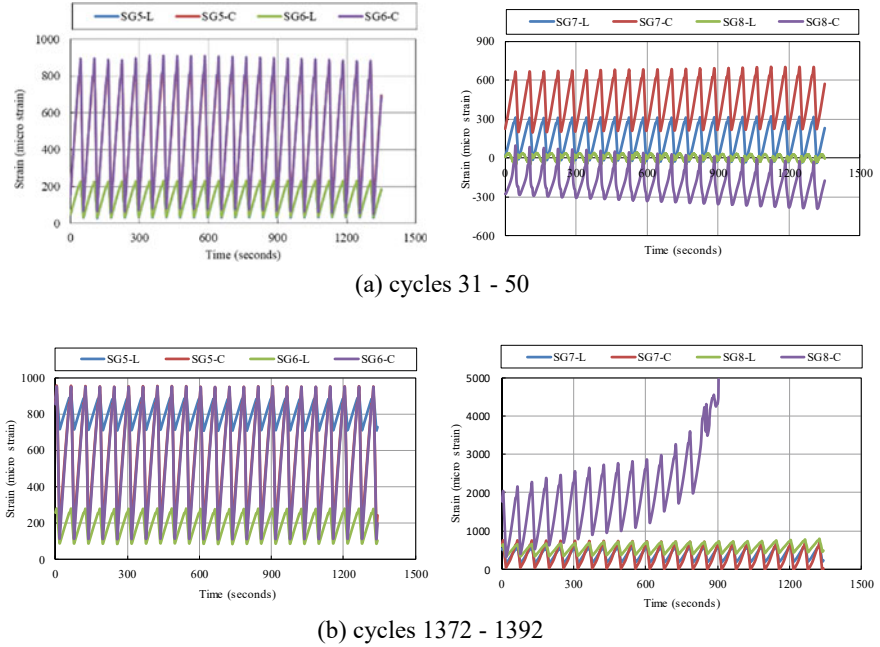
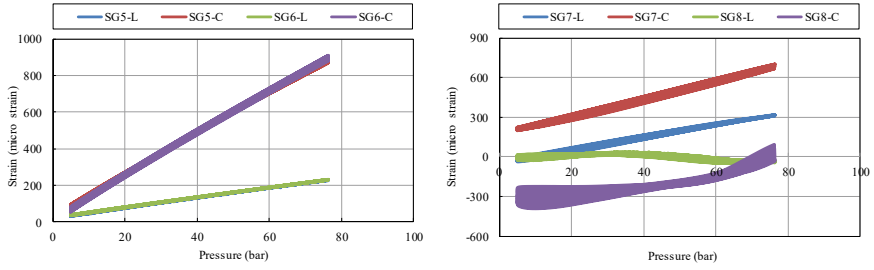


Fig. 6 Strain versus time curves for pipe specimen with longitudinal seam crack

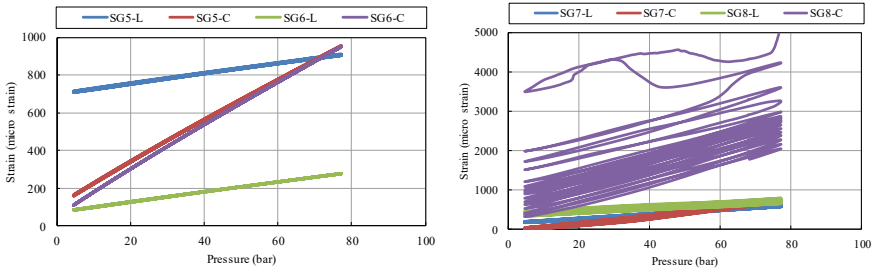
of crack. SIF values predicted using ASME B&PV Code were slightly higher than the values predicted using API 579/ASME FFS-1 both at the deepest and surface points of crack. Employing Paris' crack growth model and crack growth constants available in the literature, number of cycles to failure was predicted. The values of Paris's crack growth constants  $C$  and  $m$  used in the present studies were  $3 \times 10^{-8}$  and 2.615 respectively. The number of cycles predicted using API 579/ASME FFS-1 and ASME B&PV Code Section XI were 5264 and 1691 respectively. The number of cycles predicted with the SIF values obtained from both the approaches were un-conservative. Tiku et al. [7] compared fatigue crack growth rates obtained from full-scale tests with the existing BS 7910 and API 579 formulations. The comparison confirmed that the BS 7910 approach results in very conservative estimates of fatigue crack growth rates for axial flaws. The BS 7910 stress intensity factor formulation overestimated the bulging correction for axially oriented flaws.

## 7 Summary and Conclusions

Fatigue life studies on API 5L X46 grade steel in-service pipes of 350 mm diameter and 7.14 mm thickness subjected to cyclic internal pressure was carried out experimentally. One pipe had a longitudinal seam crack of 32 mm length and 2 mm depth

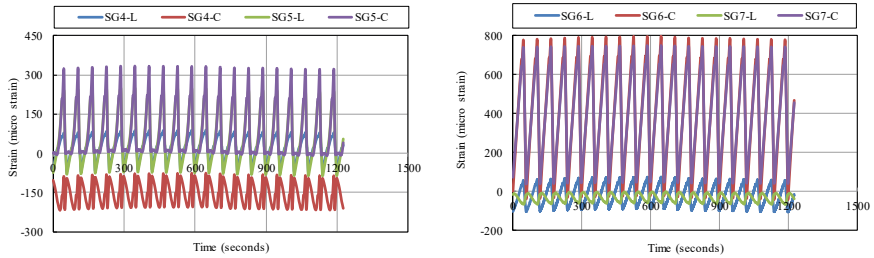


(a) cycles 31 - 50

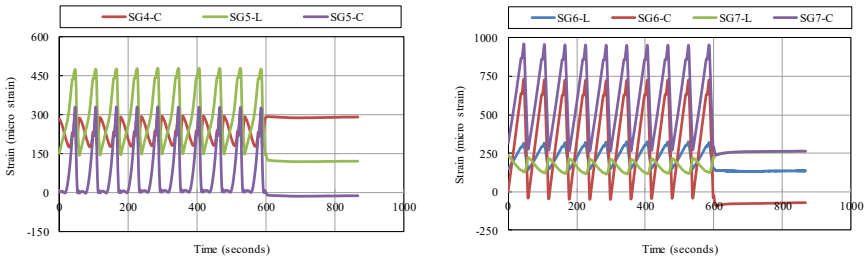


(b) cycles 1372 - 1392

Fig. 7 Strain versus pressure curves for pipe specimen with longitudinal seam crack



(a) cycles 1501 - 1520



(b) cycles 2001 - 2010

Fig. 8 Strain versus time curves for pipe specimen with lamination defects

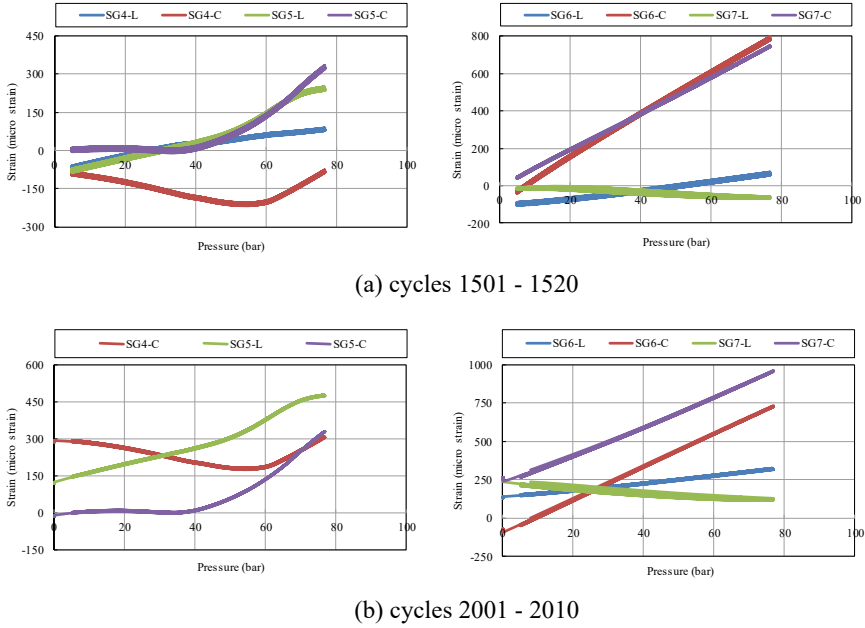


Fig. 9 Strain versus pressure curves for pipe specimen with lamination defects

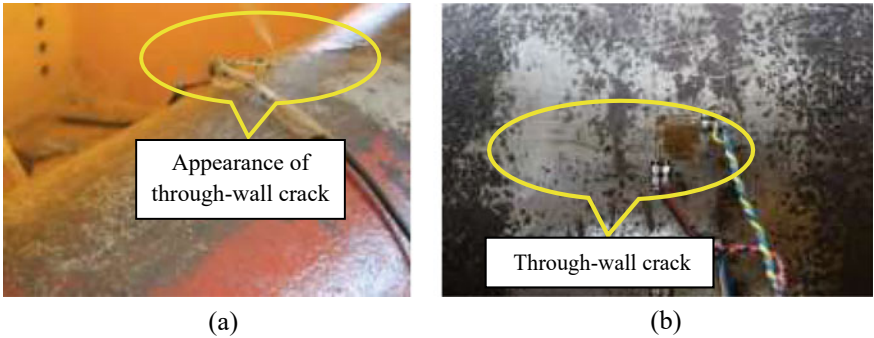
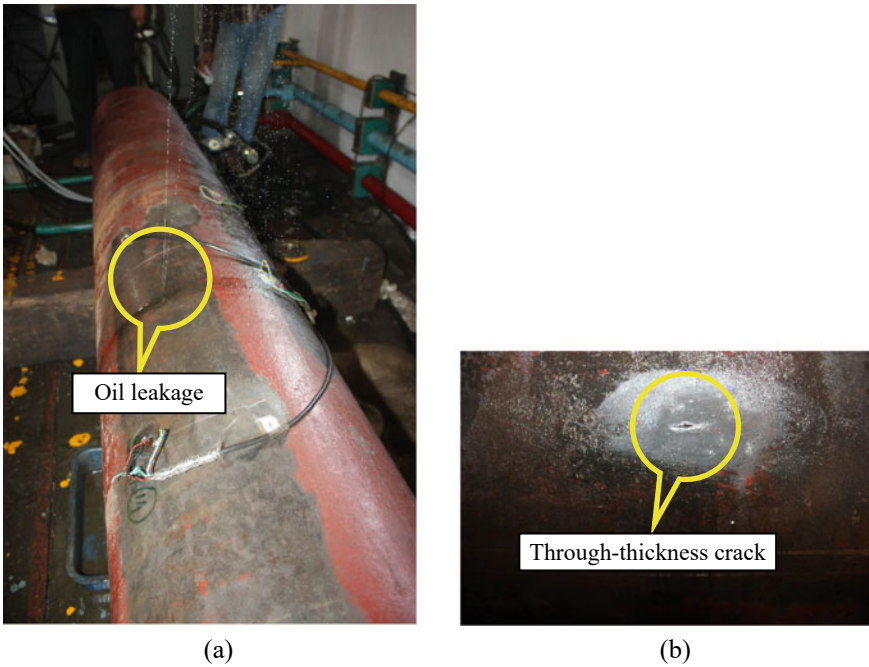


Fig. 10 Close-up views of failure of pipe specimen with longitudinal seam crack

and the other pipe had two lamination defects of different sizes. The pipe specimens were subjected to a cyclic pressure of 5–77 kg/cm<sup>2</sup> and then back to 5 kg/cm<sup>2</sup>, typically being followed in oil pipeline industry in India. The existing defects became through-wall crack and the specimens failed at 1412 and 2010 cycles, indicating 3.87 years and 5.51 years of remaining service life. Numerical studies were carried out on the pipes under cyclic internal pressure and stress intensity factor was evaluated by varying crack length and depth using domain integral technique. It was observed that the SIF is higher for the crack tip located nearer to the support than for



**Fig. 11** Close-up views of failure of pipe specimen with lamination defects



**Fig. 12** Stress distribution ahead of crack tip

the crack tip located away from the support due to the geometrical constraint effect of the crack position. SIF for different crack depths was also evaluated analytically using the expressions available in API 579/ASME FFS-1 and ASME B&PV Code Section XI Division I. SIF values predicted using ASME B&PV Code were slightly higher than the values predicted using API 579/ASME FFS-1 both at the deepest and surface points of crack. Employing Paris' crack growth model and crack growth constants reported in the literature for API 5L X46 grade steel, number of cycles to failure was predicted and the results are compared.

**Fig. 13** Stress intensity factor versus crack depth

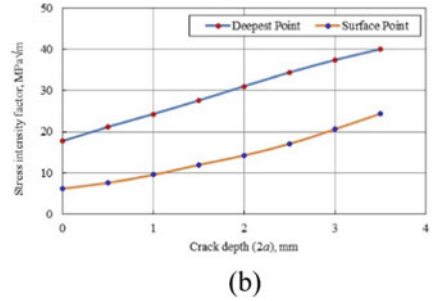
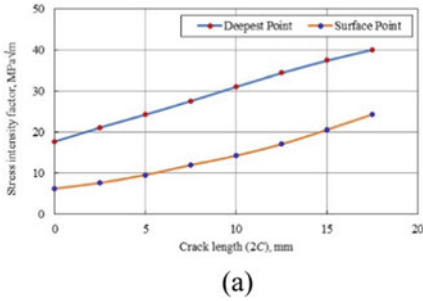
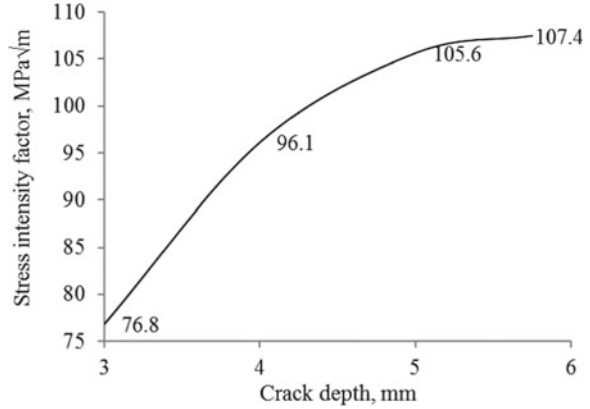


**Fig. 14** SIF prediction using API 579/ASME FFS-1

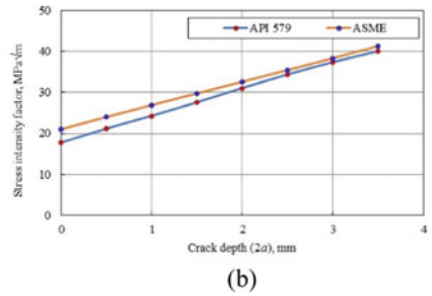
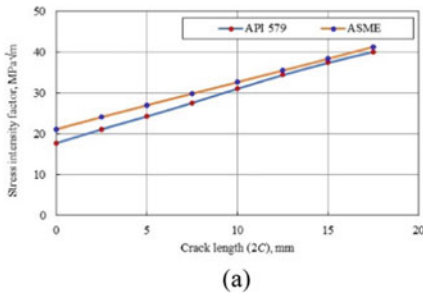


**Fig. 15** Comparison of SIF obtained from API 579/ASME FFS-1 and ASME B&PV Code Section XI Division I

## References

1. Mogila M, Davis P, Burn S (2008) Strong exploration of a cast iron pipe failure model. Reliab Eng Syst Saf 93:863–874

2. Purbolaksono J, Hong YW, Nor SSM, Othman H, Ahmad B (2009) Evaluation on reheater tube failure. *Eng Fail Anal* 16(1):533–537
3. Palmer-Jones R, Paisley D (2000) Repairing internal corrosion defects in pipelines—a case study. In: 4th International pipeline rehabilitation and maintenance conference, pp 1–25, Prague
4. Popoola LT, Grema AS, Latinwo GK, Gutti B, Balogun AS (2013) Corrosion problems during oil and gas production and its mitigation. *Int J Industr Chem* 135(4):1–15
5. Zheng M, Luo JH, Zhao XW, Bai ZQ, Wang R (2005) Effect of pre-deformation on the fatigue crack initiation life of X60 pipeline steel. *Int J Press Vessels Pip* 82:546–552
6. Azevedo CRF (2007) Failure analysis of a crude oil pipeline. *Eng Failure Anal* 14:978–994
7. Liu PF, Zheng JY, Sun GY (2010) Fatigue lifetime evaluation of buried pipeline under internal pressure and vibrating loads. *J Mech Strength* 1:125–129
8. Liu PF, Zheng JY, Zhang BJ, Shi P (2010) “Fatigue analysis of natural gas buried X65 steel pipeline under deflection load using finite element method. *Mater Des* 31:1384–1391
9. Hasan F, Iqbal J, Ahmed F (2007) Stress corrosion failure of high-pressure gas pipeline. *Eng Fail Anal* 14:801–809
10. Hajibagheri HR, Heidari A, Amini R (2018) An experimental investigation of the nature of longitudinal cracks in oil and gas transmission pipelines. *J Alloys Compd* 741:1121–1129
11. Nguyen TT, Heo HM, Park J, Nahm SH, Beak UB (2021) Fracture properties and fatigue life assessment of API X70 pipeline steel under the effect of an environment containing hydrogen. *J Mech Sci Technol* 35:1445–1455
12. Jiao Z, Shuai J (2014) A cyclic internal pressure characteristics analysis of long distance transmission pipelines. *Pet Sci Technol* 32(1):61–67
13. Ghaednia H, Das S, Zohrehheydariha J, Wang R, Kania R (2016) Effect of crack depth on burst strength of X70 pipeline with dent-crack defect. In: 11th International pipeline conference (IPC2016), Calgary (2016)
14. Tiku S, Ghovanlou M, Dinovitzer A, Piazza M, Jones TA (2020) Full scale test validation of fatigue crack growth rate of flaws in ERW pipe. In: 13th International pipeline conference, Calgary (2020)
15. Tewari AK, Agarwal D (2018) A case study: failure analysis of crude oil pipeline rupture. *Int Res J Eng Technol* 5(7):2415–2422
16. API 5L (2018) Specification for line pipe. American Petroleum Institute, 46th ed
17. API 579-1/ASME FFS-1 (2016) Fitness-for-service. API Publishing Services, Washington DC, USA
18. Rules for inservice inspection of nuclear power plant components, Section XI, Division 1, ASME Boiler and Pressure Vessel Code, 2010, New York.